



Destruction of chain superconductivity in $\text{YBa}_2\text{Cu}_4\text{O}_8$ in a weak magnetic field

A. Serafin,¹ J. D. Fletcher,¹ S. Adachi,² N. E. Hussey,¹ and A. Carrington¹

¹*H. H. Wills Physics Laboratory, University of Bristol, Tyndall Avenue, Bristol BS8 1TL, United Kingdom*

²*Superconducting Research Laboratory, International Superconductivity Technology Center, Shinonome 1-10-13, Tokyo 135, Japan*

(Received 20 August 2010; published 20 October 2010)

We report measurements of the temperature-dependent components of the magnetic penetration depth $\lambda(T)$ in single-crystal samples of $\text{YBa}_2\text{Cu}_4\text{O}_8$ using a radio-frequency tunnel diode oscillator technique. We observe a downturn in $\lambda(T)$ at low temperatures for currents flowing along the b and c axes but not along the a axis. The downturn in λ_b is suppressed by a small dc field of ~ 0.25 T. This and the zero field anisotropy of $\lambda(T)$ likely result from proximity induced superconducting on the CuO chains. However we also discuss the possibility that a significant part of the anisotropy might originate from the CuO_2 planes.

DOI: [10.1103/PhysRevB.82.140506](https://doi.org/10.1103/PhysRevB.82.140506)

PACS number(s): 74.72.Gh

The Y-based high- T_c cuprate superconductors are unique in that they have quasi-one-dimensional CuO chain structures in addition to the CuO_2 planes in which the interactions responsible for superconductivity are thought to originate. The effect of these chain layers on the normal and superconducting state properties has long been debated. Indeed, since the Y-based cuprates are so far the only hole-doped cuprates which show quantum oscillations in their underdoped state,¹⁻³ it is natural to question if the coherent electron orbits could in fact originate in the chain parts of the Fermi surface (FS).^{4,5} An important question is whether the chain FS is superconducting and if so is this superconductivity quenched by a much smaller magnetic field than the plane.

$\text{YBa}_2\text{Cu}_3\text{O}_{7-\delta}$ (Y-123) contains a single CuO chain per unit cell whose oxygen content can be varied to tune the doping level on the CuO_2 plane. Its close relative $\text{YBa}_2\text{Cu}_4\text{O}_8$ (Y-124) has a double chain layer that is stoichiometric and a planar state that is slightly underdoped.² According to band-structure calculations^{4,6,7} the chains form quasi-one-dimensional (1D) electronic bands which cut across the CuO_2 plane FS sheets, with considerable hybridization between the states close to the crossing points. As the electron-pairing interaction which gives rise to superconductivity in the cuprates is likely to rely strongly on the electronic structure of the quasi-two-dimensional (2D) plane, it might seem unlikely that there is any intrinsic pairing of electrons on the chain. Indeed, in isostructural Pr-124, the double chain network is metallic yet exhibits no superconductivity down to 0.5 K.⁸

In both Y-123 and Y-124, the CuO chains have been modeled as an essentially normal layer which is coupled to the planes via single electron tunnelling, similar to the classical proximity effect between normal metals and superconductors.^{9,10} This is augmented by the strong hybridization between plane and chain states which occurs at certain momentum values. The model predicts that the chain states will have low-energy gap structures arising from variations of the gap within the chain FS. This implies that the superfluid density should have quite different temperature dependencies for screening currents flowing in the a or b (chain) directions. Experimentally however, it is found that for Y-123 the temperature dependence of λ_a and λ_b are very similar^{11,12} although their zero temperature values differ.^{13,14}

This has led to the proposal that there are intrinsic pairing interactions on the chains and that the planes and chains are predominately coupled by Josephson-type pair tunnelling.¹⁰ Alternatively, this has been explained by chain disorder.¹⁵

In this Rapid Communication, we report measurements of the anisotropic components of the magnetic penetration depth in Y-124 single crystals as a function of temperature and dc field. A rapid suppression of the superconducting component on the CuO double chain is observed in a small applied field. These results are significantly different to those obtained on optimally doped Y-123 and appear to support the proximity effect model for Y-124. However, some questions remain.

Single crystals of $\text{YBa}_2\text{Cu}_4\text{O}_8$ were grown using a high oxygen pressure flux based method.¹⁶ Penetration depth was measured using a radio-frequency (RF) tunnel diode oscillator method¹² operating at ~ 12 MHz. The sample is attached with vacuum grease to a sapphire rod and is placed in a copper coil which forms part of the oscillator's tank circuit. A small superconducting solenoid allows us to apply a dc field colinear with the weak RF probe field ($H_{\text{RF}} \approx 10^{-6}$ T).

Changes in the resonant frequency of our RF oscillator ΔF are directly proportional to changes in sample's superconducting volume as a function of temperature or field. The samples are thin platelets with dimensions $\ell_{a,b,c}$ along the respective crystallographic directions (Fig. 1). With the RF field applied along the b direction the change in frequency ΔF due to changes in the λ_a and λ_c is given by $\Delta F = 2\alpha\beta(\ell_a\ell_b\Delta\lambda_a + \ell_b\ell_c\Delta\lambda_c)$ where α is a constant set by the coil geometry and β is the effective sample demagnetizing factor.¹⁷ Hence, contributions from two components of λ are always mixed. In principle, it is possible to separate the components by making measurements of $\Delta\lambda$ with H_{RF} in all three directions, however in practice this approach is inaccurate because of uncertainties in the demagnetizing factor particularly in the $H\parallel c$ configuration. Instead, we cleaved the sample (using a razor blade) halving ℓ_a and thus doubling the contribution of $\Delta\lambda_c$ in the $H\parallel b$ configuration.¹⁸ Measurements of sample 1 with $H\parallel b$ (where the demagnetising effect is small) before and after cleaving thus allow us to isolate the λ_c contribution which then can be subtracted from the measurements with $H\parallel a$ and $H\parallel b$ to yield the three components of λ . Cleaving the sample a second time resulted in consis-

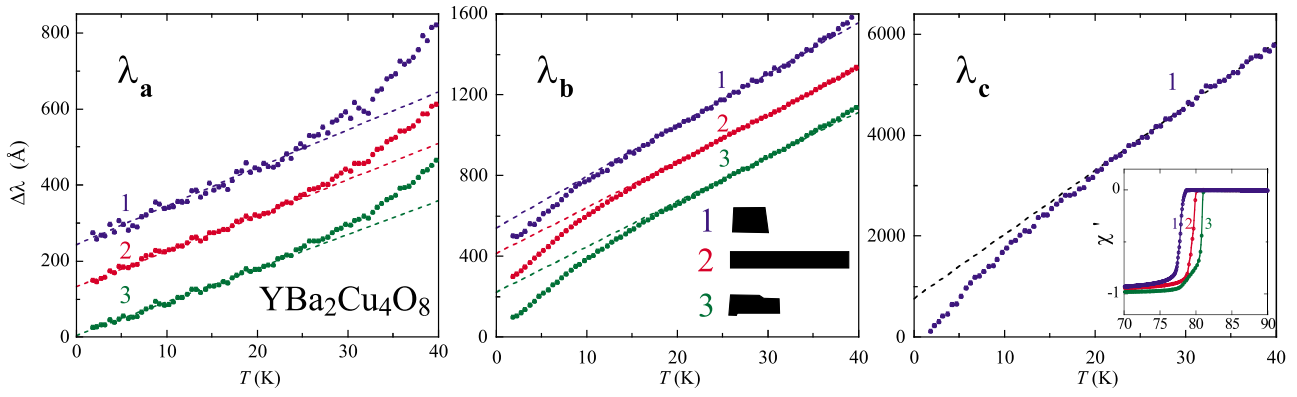


FIG. 1. (Color online) Temperature dependence of the penetration depth for the three principle directions for $\text{YBa}_2\text{Cu}_4\text{O}_8$. The shapes of the samples are shown in the λ_b panel. Their dimensions ($\ell_a \times \ell_b \times \ell_c$) are: sample 1: $115 \times 80 \times 15 \mu\text{m}^3$, sample 2: $60 \times 420 \times 8 \mu\text{m}^3$, and sample 3: $170 \times 60 \times 6 \mu\text{m}^3$. The RF susceptibility (χ') close to T_c (normalized to -1 at low temperature) is shown in the λ_c panel.

tent behavior [$\Delta\lambda_c(T=30 \text{ K})$ was the same to within $\sim 10\%$]. The extracted $\Delta\lambda_c(T)$ was used to extract $\Delta\lambda_a(T)$ and $\Delta\lambda_b(T)$ from two further samples (see Fig. 1). The consistency of results for these samples which have different contributions from λ_c shows that $\Delta\lambda_c(T)$ was accurately determined.

The temperature dependence of the three extracted components of λ below $T=40 \text{ K}$ are shown in Fig. 1. λ_a has a linear T dependence from base temperature up to $\sim 25 \text{ K}$ with slope $d\lambda_a/dT=9.6(6) \text{ \AA}/\text{K}$ which is consistent with a simple d -wave model.¹⁹ The behavior of $\Delta\lambda_b$ and $\Delta\lambda_c$ are quite different to $\Delta\lambda_a$. Between ~ 15 and 30 K $\Delta\lambda_b(T)$ is linear with a slope $d\lambda_b/dT=24(2) \text{ \AA}/\text{K}$ which is ~ 2.5 times larger than for λ_a . Below $T \sim 15 \text{ K}$ however, there is a downturn in $\Delta\lambda_b(T)$ which indicates the onset of additional screening which reduces λ_b by $\sim 150 \text{ \AA}$ at $T=2 \text{ K}$ compared to the extrapolated linear behavior. Similar behavior is found for $\Delta\lambda_c$, where the downturn sets in at approximately the same temperature and $d\lambda_c/dT=130 \text{ \AA}/\text{K}$. A downturn in $\lambda(T)$ had been seen in previous measurements of Y-124 (Refs. 20 and 21) however the separate contributions of λ_a and λ_b were not determined.

In the conventional model of d -wave superconductivity¹⁹ with a circular 2D FS we expect $\frac{d\lambda}{dT} = \frac{2 \ln 2 \lambda(0)}{d\Delta/d\phi|_{\text{node}}}$. We cannot measure $\lambda(0)$ directly in our experiments. However, infrared reflectivity (IRR) experiments¹³ on Y-124 give $\lambda_a(0) = 2000 \text{ \AA}$ and $\lambda_b(0) = 800 \text{ \AA}$, (the anisotropy $\lambda_a/\lambda_b = 2.5$). Although the λ anisotropy measured by IRR for Y-123 ($\lambda_a/\lambda_b \approx 1.6$) is somewhat higher than that measured by other other techniques ($\lambda_a/\lambda_b \approx 1.2$) (Ref. 14) it does seem likely that λ_a/λ_b is significantly greater than unity for Y-124 which is in the opposite direction to our measured anisotropy in $d\lambda/dT$. Hence, Fermi velocity anisotropy alone cannot explain the data within this simple model. If the order parameter had a significant s component (i.e., $d + \eta s$) so that the nodes move away from $\phi=45^\circ$ toward the b direction, then the paramagnetic current produced by the thermally excited nodal quasiparticles could be larger in the b direction and this, in principle, could overcome the opposite anisotropy of $\lambda(0)$. Within a single band model a value of $\lambda_a/\lambda_b = 2.5$ implies a substantial anisotropy of the in-plane Fermi velocity. Calculations based on fits to photoemission results²² how-

ever, suggest that at a doping level of $p=0.14$ the anisotropy of the in-plane superfluid density is only $\sim 2\%$.

An explanation for both the larger value of $\lambda(0)$ and $\Delta\lambda(T)$ in the b direction can be found in the plane-chain proximity models mentioned above. In Fig. 2 we show the normalized superfluid density $\rho = \lambda(0)^2 / [\lambda(0) + \Delta\lambda(T)]^2$ for sample 2, calculated using the values of $\lambda(0)$ taken from infrared measurements¹³ (λ_a and λ_b) and aligned polycrystalline measurements (λ_c).²³ The behavior in the a direction is similar to that found for ρ_a and ρ_b of Y-123, and varies linearly with T up to $\sim T_c/2$. However, both $\rho_b(T)$ and $\rho_c(T)$ are quite different with both showing strong upward curvature for temperature below $\sim T_c/3$. In contrast, in Y-123, $\rho_b(T)$ is similar to $\rho_a(T)$ and $\rho_c(T)$ has a much weaker temperature

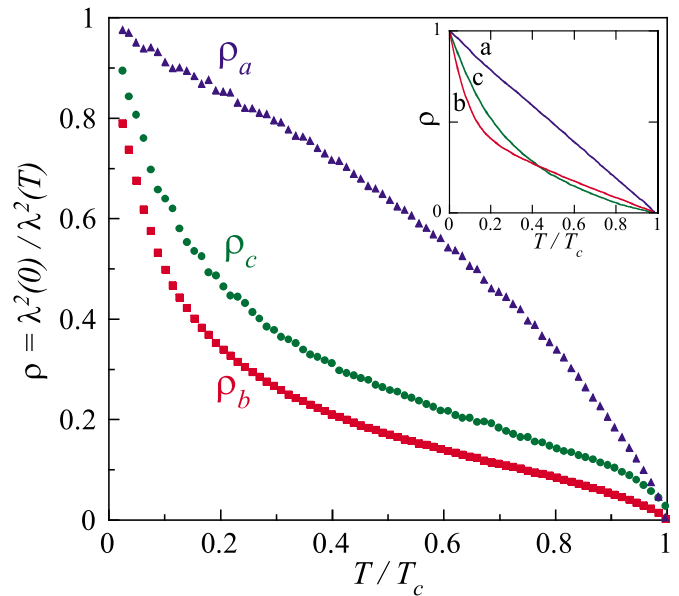


FIG. 2. (Color online) Normalized superfluid density $\rho = [\lambda(0)^2 / [\lambda(0) + \Delta\lambda(T)]^2]$ for sample 2 in all three directions using values of $\lambda(0)$ taken from infrared measurements (Ref. 13) [$\lambda_a(0) = 2000 \text{ \AA}$ and $\lambda_b(0) = 800 \text{ \AA}$] and aligned polycrystalline measurements [$\lambda_c(0) = 6150 \text{ \AA}$] (Ref. 23). The inset shows theoretical predictions for ρ in the proximity coupling (single electron tunneling) model taken from Ref. 10.

dependence than both in-plane components at low T .¹⁸ The small downturn in $\Delta\lambda_b(T)$ below 15 K noted above (Fig. 1) is not the primary reason for the disparity between ρ_a and ρ_b in Y-124; rather it is caused by the substantial difference in the ratio $(d\lambda/dT)/\lambda(0)$ which is $4.8 \times 10^{-3} \text{ K}^{-1}$ for the a axis but ~ 6 times larger ($30 \times 10^{-3} \text{ K}^{-1}$) for the b axis. Clearly small uncertainties in the values of $\lambda(0)$ will not have a large effect on this. These upturns are similar to those reported for the average in-plane and c axis superfluid density measured on polycrystalline samples.²³

In the inset to Fig. 2 we show the predictions of the single electron tunnelling plane-chain proximity coupling model of Ref. 10 (similar results using a similar model are also given in Ref. 9). These predictions are very similar to our experimental findings, with both $\rho_b(T)$ and $\rho_c(T)$ having strong upward curvature below $\sim T_c/3$. In this particular simulation both plane and chain FS were assumed to be superconducting but similar results are found when there is no intrinsic gap on the chains.⁹ A feature of this proximity model is that the upward curvature of ρ_b is strongly suppressed by impurity scattering (e.g., broken chain segments).¹⁵ The difference between Y-123 and Y-124 may then be due to fact that Y-124 has completely full chains whereas in Y-123 the chain segments are much shorter (more disorder). Interchain coupling in Y-124 will reduce localization effects which are likely to be present in the more 1D Y-123 chains.

Next we discuss the field dependence of λ . Here we apply a dc field colinear with the RF probe field along the c direction where H_{c1} is maximal. Data for sample 2 are shown in Fig. 3 for dc fields up to 50 mT. In this field configuration the measured $\Delta\lambda_{ab}$ is a mixture of $\Delta\lambda_a$ and $\Delta\lambda_b$ but because of the aspect ratio of this particular sample ($\ell_b/\ell_a \approx 5$) around 80% of $\Delta\lambda_{ab}$ comes from $\Delta\lambda_b$. In this configuration the calibration factor is difficult to calculate (especially for a sample with such an elongated shape), so we determined it experimentally by measuring, in both the $H\parallel ab$ and $H\parallel c$ configurations, a twinned sample of Y-123 with almost identical shape. From the total frequency shifts measured when the sample was withdrawn from the coil and from the sample dimensions we estimate that the demagnetizing field enhancement factor $\beta \approx 5$ hence the effective surface fields are 5 times larger than the applied field.

For $H_{dc}=0$ (Fig. 3) a strong downturn in $\lambda_{ab}(T)$ is seen below $T \approx 15$ K as in the direct measurements of $\Delta\lambda_b(T)$ (Fig. 1). As H_{dc} is increased, initially there is no change and then at $\mu_0 H_{dc} \approx 5$ mT, $\lambda_b(T=2 \text{ K})$ starts to increase monotonically and eventually saturates for $\mu_0 H_{dc} \gtrsim 50$ mT (see inset Fig. 3). The temperature dependence of λ_{ab} also changes, from $\sim T^{0.7}$ for $H_{dc}=0$ to $\sim T^{1.2}$ for $\mu_0 H_{dc}=50$ mT. The applied dc field wipes out the downturn in λ_{ab} and returns the temperature dependence to a quasilinear variation expected from a conventional d -wave superconductor with small amounts of impurities.²⁴ Similar behavior with comparable field scales was observed in two other samples.²⁰ The high field behavior of $\lambda_{ab}(T)$ (and hence λ_b) is less linear than λ_a at the lowest temperatures. A similar difference is also found in Y-123 (Ref. 18) and could result from anisotropic impurity scattering.

For $\mu_0 H_{dc} \lesssim 35$ mT $\Delta\lambda_{ab}$ is perfectly reversible on cycling from base temperature (where the field was increased)

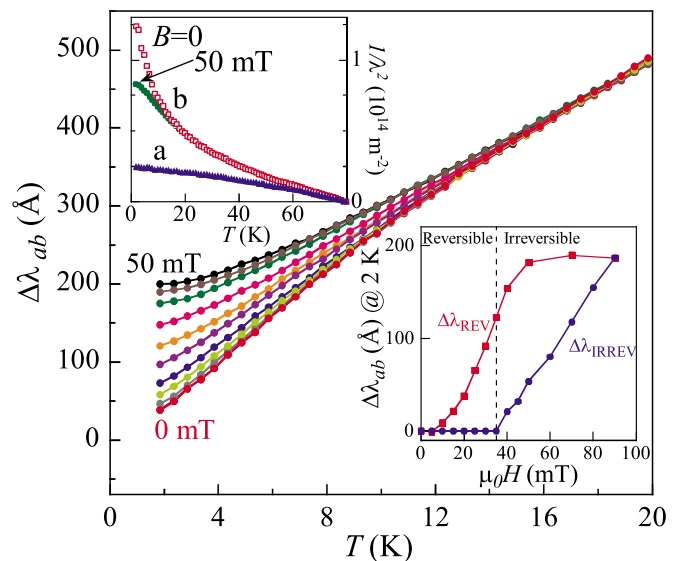


FIG. 3. (Color online) Field dependence of λ_{ab} for sample 2 (dimensions $60 \times 300 \times 8 \mu\text{m}^3$) from 0 to 50 mT in 5 mT increments. The b -axis dimension is less than that stated in Fig. 1 because it was broken between runs. The aspect ratio of this sample means that $\sim 80\%$ of λ_{ab} comes from λ_b . To remove artifacts arising from the field dependent (but temperature independent) background from the measurement coil the data have been shifted in frequency so that they coincide at $T=20$ K for all fields. The lower inset shows the change in λ at the fixed temperature of 2 K along with the irreversible changes to λ_{ab} , showing the onset of flux entry at ~ 35 mT. The upper inset shows the superfluid density along a and b axes in zero field together with the b axis data in 50 mT. Here $\Delta\lambda_b(T)$ at 50 mT has been approximated by $1.2\Delta\lambda_{ab}$. The factor 1.2 accounts for the small contribution of λ_a to λ_{ab} .

up to 20 K and back again. For fields above this $\Delta\lambda_{ab}(T)$ was hysteretic on the first temperature cycle and then reversible thereafter. This irreversibility increased linearly with field (see inset Fig. 3). We attribute this hysteresis to vortex motion. Initially, as the vortices enter the sample they are not in deep pinning wells and so give a strong contribution to the measured effective λ . Upon temperature cycling they settle on strong pinning sites (or move to the center of the sample) and therefore no longer give a strong contribution to $\lambda(T)$. As the field at which $\lambda_{ab}(T)$ begins to change is far below the field at which the hysteretic behavior set in, and since for fields greater than this the reversible part of $\Delta\lambda(H)$ begins to saturate whereas the irreversible part increases linearly with H , it is clear that vortex motion is not responsible for the changes in the reversible part of $\Delta\lambda_{ab}(H)$ which are shown in the main part of Fig. 3. Rather, the reversible changes reflect the field dependence of the London component to $\lambda(T)$. Direct measurements of the dc magnetization using a superconducting quantum interference device magnetometer showed that the field of first flux penetration (which is likely considerably larger than H_{c1}) was ~ 35 mT, for this sample and field configuration at $T=10$ K, which coincides with the onset of irreversibility. If the field dependence of $\Delta\lambda_{ab}$ was interpreted in terms of vortex motion it would be difficult to understand why the vortex contribution saturates at higher field, sets in at exactly the point where the downturn in

$\Delta\lambda_b(T)$ starts at 15 K, and increases with field and temperature such that it makes $\Delta\lambda_{ab}$ linear in temperature at the point at which the field dependence saturates. On the other hand, if the changes originate from the field dependence of the London penetration depth then all these facts can be simply understood.

Field dependence of λ in the Meissner state can result from several effects. A linear increase of λ with H is expected from Doppler shifted quasiparticles close to the nodal points.¹⁹ This effect is however, very small (~ 2 Å for $\mu_0 H = 10$ mT for Y-123) and has never been conclusively observed [the measured $\lambda(H)$ in Y-123 does not have the temperature or field orientation dependence expected from theory and may therefore have another origin].^{12,25} A decrease in λ with increasing field can also result from the presence of Andreev bound states²⁶ but this is in the opposite direction to what is observed here.

Instead, the most likely explanation is that in Y-124 the small dc field quenches at least part of the superconducting current in the chains. We might expect this to occur when the Doppler shift of the chain quasiparticle energies are of order the chain gap. It is often observed that proximity-driven superconductivity is quenched in small fields,²⁷ for example, the π band superconductivity in MgB₂.²⁸ In Y-124 the magnetic field does not affect $\lambda(T)$ above ~ 15 K and the strong anisotropy in $d\lambda/dT$ between the a and b direction as discussed above remains. Also the field induced change in $\lambda_{ab} \approx 190$ Å at the lowest temperature which does not significantly change the anisotropy of λ . This is illustrated in the inset to Fig. 3 where we show the field suppressed superfluid density along the b axis along with the zero field results.

The fact that only part of the excess b axis superfluid (relative to the a axis) is suppressed in weak field (~ 0.25 T including demagnetizing effects) might suggest that there is significant variation of the gap along the chain FS.²⁹ If the system is sufficiently clean, so that scattering between regions of the chain FS with different gaps (resulting from a variation in the plane-chain hybridization) is small, then the downturn in $\lambda_b(T)$ and $\lambda_c(T)$ for $T \lesssim 15$ K could result from a region of chain FS with weak pairing becoming superconducting. This region then becomes normal when a weak field is applied. Alternatively, the downturn and field dependence could reflect the superconductivity in the chain as a whole and then the remaining anisotropy in high field would reflect the anisotropy of the CuO₂ planes. Although, as mentioned above, there is no indication of such anisotropy from photoemission experiments we note that quantum oscillation^{2,3} and magnetotransport³⁰ measurements show that there is a significant reconstruction of the FS in this material at low temperature. Recently, evidence of significant electronic anisotropy in the CuO₂ planes of underdoped Y-123 has been found in Nernst effect measurements³¹ and it is likely that properties of Y-124 are similar. Further theoretical work calculating the effect of magnetic field on the superfluid density in the proximity models^{9,10} would help decide between these two competing interpretations. Completing the picture of plane-chain superconductivity in Y-124 and Y-123 should help our understanding of quantum oscillations and the underlying electronic structure of these materials.

We thank Francisco Manzano and Ruslan Prozorov for their contributions to this project and David Broun and Bill Atkinson for useful discussions. This work was funded by the UK EPSRC.

¹N. Doiron-Leyraud *et al.*, *Nature (London)* **447**, 565 (2007).

²A. F. Bangura *et al.*, *Phys. Rev. Lett.* **100**, 047004 (2008).

³E. A. Yelland *et al.*, *Phys. Rev. Lett.* **100**, 047003 (2008).

⁴A. Carrington and E. A. Yelland, *Phys. Rev. B* **76**, 140508 (2007).

⁵S. C. Riggs *et al.*, [arXiv:1008.1568](https://arxiv.org/abs/1008.1568) (unpublished).

⁶C. Ambrosch-Draxl *et al.*, *Phys. Rev. B* **44**, 5141 (1991).

⁷J. J. Yu *et al.*, *Physica C* **172**, 467 (1991).

⁸N. E. Hussey *et al.*, *Phys. Rev. Lett.* **89**, 086601 (2002).

⁹W. A. Atkinson and J. P. Carbotte, *Phys. Rev. B* **52**, 10601 (1995).

¹⁰T. Xiang and J. M. Wheatley, *Phys. Rev. Lett.* **76**, 134 (1996).

¹¹K. Zhang *et al.*, *Phys. Rev. Lett.* **73**, 2484 (1994).

¹²A. Carrington *et al.*, *Phys. Rev. B* **59**, R14173 (1999).

¹³D. N. Basov *et al.*, *Phys. Rev. Lett.* **74**, 598 (1995).

¹⁴R. F. Kiefl *et al.*, *Phys. Rev. B* **81**, 180502 (2010).

¹⁵W. A. Atkinson, *Phys. Rev. B* **59**, 3377 (1999).

¹⁶S. Adachi *et al.*, *Physica C* **301**, 123 (1998).

¹⁷Here we neglect the small contribution from the currents on small sample surfaces perpendicular to the field.

¹⁸D. A. Bonn *et al.*, *Czech. J. Phys.* **46**, 3195 (1996).

¹⁹D. Xu *et al.*, *Phys. Rev. B* **51**, 16233 (1995).

²⁰F. Manzano, Ph.D. thesis, University of Bristol, 2002.

²¹G. Lamura *et al.*, *J. Phys. Chem. Solids* **67**, 447 (2006).

²²T. Kondo *et al.*, *Phys. Rev. B* **80**, 100505 (2009).

²³C. Panagopoulos *et al.*, *Phys. Rev. B* **59**, R6635 (1999).

²⁴P. J. Hirschfeld and N. Goldenfeld, *Phys. Rev. B* **48**, 4219 (1993).

²⁵C. P. Bidinosti *et al.*, *Phys. Rev. Lett.* **83**, 3277 (1999).

²⁶A. Carrington *et al.*, *Phys. Rev. Lett.* **86**, 1074 (2001).

²⁷R. Prozorov *et al.*, *Phys. Rev. B* **64**, 180501 (2001).

²⁸F. Bouquet *et al.*, *Phys. Rev. Lett.* **89**, 257001 (2002).

²⁹W. A. Atkinson, *Supercond. Sci. Technol.* **22**, 014005 (2009).

³⁰P. M. C. Rourke *et al.*, *Phys. Rev. B* **82**, 020514 (2010).

³¹R. Daou *et al.*, *Nature (London)* **463**, 519 (2010).